Nonlinear Effect on Focusing Gain of a Focusing Transducer with a Wide Aperture Angle *

LIU Ming-He(柳鸣鹤), ZHANG Dong(章东)**, GONG Xiu-Fen(龚秀芬)

Lab of Modern Acoustics, Institute of Acoustics, Nanjing University, Nanjing 210093

(Received 17 January 2007)

Nonlinear effect on focusing gain of acoustic field radiated from a 1-MHz focusing transmitter with a wide aperture angle of 35° is theoretically and experimentally investigated. With the enhancement of nonlinearity, the focusing gains of both intensity and peak positive pressure show non-monotonic behaviour. There exist the same saturated levels at which the maximum outputs are reached and their spatial distributions are more localized. In contrast, the peak negative pressure always decreases monotonically and its spatial distribution is less localized.

PACS: 43. 80. +p, 43. 25. +y

High-intensity focused ultrasound (HIFU) is a noninvasive treatment that focuses high-intensity ultrasound energy to the targeted area of tissues within the body without damage to intervening tissues. The principle of this technique is to raise the tissue temperature to be relatively high and to cause thermal coagulation and ablation of cells by using an ultrasonic focusing transducer.[1,2] Recently, research of the transducer with a wide aperture angle has been paid much attention owing to its advantage of keeping high ultrasonic intensity for a few seconds to reach a necessary thermal dose.[3,4] As we know, when ultrasonic transducers are driven to produce high focal intensities in biological tissues, the sound wave is influenced by nonlinear propagation. The amplification factor of HIFU systems strongly depends on the combined effects of diffraction and nonlinearity. Nonlinear enhancement of the peak positive pressure and intensity amplification factor at the focus compared to the linear case can be observed at moderate source output. For higher source output, a nonlinear saturation phenomenon is caused by effective absorption of acoustic energy at the shocks on the focus. Most previous studies employed the Khokhlov–Zabolotskaya–Kuznetsov (KZK) nonlinear equation to quantitatively describe the nonlinear enhancement of focusing gain and saturation level at the focus for a weak focused ultrasound beam.[5–8] So far, there has been no reported result that includes the combined effect of diffraction and nonlinearity on the focal area for a strongly focused ultrasound beam. In this Letter, we quantify the importance of nonlinear effect and subsequent spatial distributions of peak positive pressure, peak negative pressure and intensity created by a strongly focused transducer based on the solution of nonlinear spheroidal beam equation (SBE) in the frequency domain.[3] The validity of the numerical calculation is examined by the measurement.

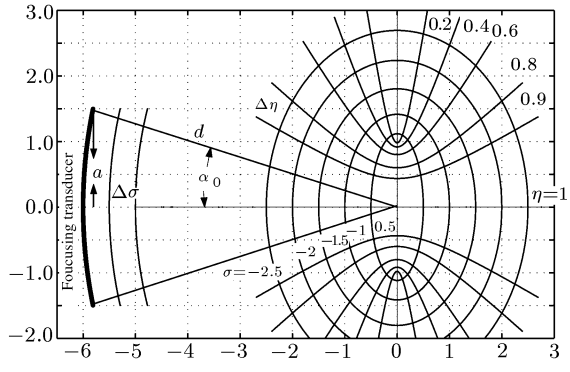

Fig. 1. Illustration of focused transducer in the oblate spheroidal coordinate system.

As shown in Fig. 1, a strong focusing transmitter with 78 mm aperture diameter and 68 mm radius of curvature (aperture angle 35°) operating at the central frequency 1 MHz is utilized in the numerical calculation and measurement. To describe the sound propagation radiated from the transmitter, we employ the nonlinear spheroidal beam equation (SBE) in an oblate spheroidal coordinate system.[3] The focused ultrasound field is divided into two regions, i.e. $\sigma < \sigma_0$ and $\sigma \geq \sigma_0$, where σ_0 denotes a specific transition location, and $\sigma_0 < 0$. The former is close to the source where spherically converging waves are predominant and the spherical coordinates are preferable; the latter is near the focus where the paraxial or planar parabolic approximation is useful. Two separated equations are used to describe the spheroidal wave and the planar wave in the two regions, respectively.

$$\frac{\partial^2 \bar{p}}{\partial \tau_s \partial \sigma} + \frac{1}{2}\frac{\sin(2\theta)}{\sigma(1+\sigma^2)}\frac{\partial^2 \bar{p}}{\partial \tau_s \partial \theta} + \frac{\varepsilon\sqrt{\sigma^2+\sin^2\theta}}{\sigma(1+\sigma^2)}\left(\frac{\partial^2 \bar{p}}{\partial \theta^2} + \cot\theta\frac{\partial \bar{p}}{\partial \theta}\right) + \frac{E}{\sigma}\frac{\partial \bar{p}}{\partial \tau_s}$$

* Supported by the Project for New Century Excellent Talents in University, and the National Natural Science Foundation of China under Grant No 10474044.

** Email: dzhang@nju.edu.cn

©2007 Chinese Physical Society and IOP Publishing Ltd

$$= \frac{\sqrt{\sigma^2+\sin^2\theta}}{\sigma}\Big(\alpha b\frac{p^3\bar{p}}{\partial\tau_s^3}+\frac{b}{2l_D}\frac{\partial^2\bar{p}^2}{\partial\tau_s^2}\Big)E, \quad (1)$$

$$\frac{\partial^2\bar{p}}{\partial\tau_p\partial\sigma}-\frac{\sigma\sin\theta}{1+\sigma^2}\frac{\partial^2\bar{p}}{\partial\tau_p\partial\theta} - \frac{\varepsilon(2-\cos\theta)}{1+\sigma^2}\Big(\frac{\partial^2\bar{p}}{\partial\theta^2}+\cot\theta\frac{\partial\bar{p}}{\partial\theta}\Big)+\frac{E}{\sigma}\frac{\partial\bar{p}}{\partial\tau_s}$$
$$= \Big(\alpha b\frac{p^3\bar{p}}{\partial\tau_p^3}+\frac{b}{2l_D}\frac{\partial^2\bar{p}^2}{\partial\tau_p^2}\Big)E, \quad (2)$$

where the variables (σ,η,φ) in the oblate spheroidal coordinate with $-\infty<\sigma<+\infty$, $0\le\eta\le 1$ and $0\le\varphi<2\pi$ are related to the rectangular coordinate (x,y,z) with $x=b[(1+\sigma^2)(1-\eta^2)]^{1/2}\cos\varphi$, $y=b[(1+\sigma^2)(1-\eta^2)]^{1/2}\sin\varphi$ and $z=b\sigma\eta$, in which $2b$ is the interfocal length. The angle variable θ is related to η as $\eta=\cos\theta$. The character ε is set to be $1/2kb$ and E is as functions of σ and θ, $E(\sigma,\theta)=(\sigma^2+\cos^2\theta)/(1+\sigma^2)$; $\tau_s=\omega[t+b(\sigma^2+\sin^2\theta)^{1/2}/c_0]$ is the spherically retarded time near the source; $\tau_p=\omega[t-b\sigma\cos\theta/c_0]$ is the retarded time for the a planar wave near the focus; $\bar{p}=p/p_0$ is the normalized sound pressure with p_0 being the amplitude of sound pressure on the source surface; c_0 is the sound speed; ρ_0 is the density of medium; β is the nonlinear coefficient of medium; k is the wave number; $l_d=\rho_0c_0^3/\beta p_0\omega$ is the shock formation distance for a planar wave; $\alpha=\delta\omega^2/2c_0^3$ is the sound attenuation coefficient with δ being the sound diffusivity and ω the angular frequency. Equations (1) and (2) are employed respectively in the regions $\sigma<\sigma_0$ and $\sigma\ge\sigma_0$. The solutions of these two equations are equal when $\sigma=\sigma_0$.

In the frequency domain, the sound pressures near the source and the focus could be reconstructed with the following Fourier series expansions, respectively:

$$\bar{p}=\sum_{n=-\infty}^{\infty}C_n^{(s)}\exp(-in\tau_s),\quad \sigma<\sigma_0<0, \quad (3)$$

$$\bar{p}=\sum_{n=-\infty}^{\infty}C_n^{(p)}\exp(-in\tau_p),\quad \sigma_0\le\sigma, \quad (4)$$

where $C_n^{(s)}$ and $C_n^{(p)}$ are the complex amplitudes of the nth harmonic. When the Fourier series is applied to Eqs. (1) and (2), we can numerically calculate the complex amplitudes $C_n^{(s)}$ and $C_n^{(p)}$, respectively. In the numerical calculation, the boundary condition at $\sigma=-\sigma_{\max}$ is given by

$$c_1^{(s)}=h^{(s)}\cos\tau_s+ig^{(s)}\sin\tau_s, \quad (5)$$

$$c_1^{(p)}=h^{(p)}\cos\tau_p+ig^{(p)}\sin\tau_p, \quad (6)$$

where $g^{(s)}=\begin{cases}1 & (0\le\theta\le\theta_0)\\ 0 & \Big(\theta_0\le\theta\le\dfrac{\pi}{2}\Big)\end{cases}$ and $h^{(s)}=0\ \Big(0\le\theta\le\dfrac{\pi}{2}\Big)$.

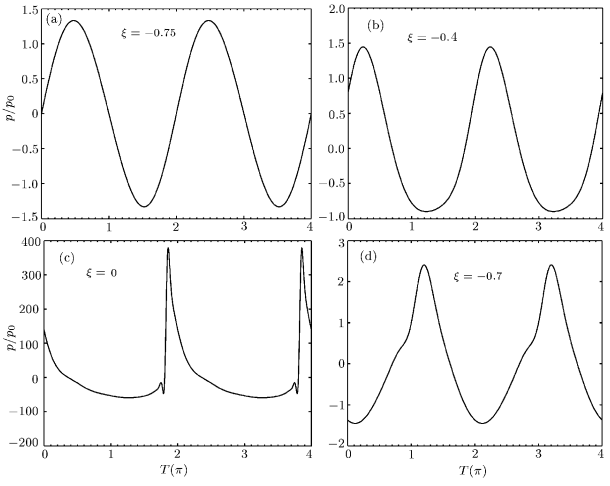

Fig. 2. Waveforms at various distances in the sound axis.

The 1-MHz focusing transmitter with a wide aperture angle 35° shown in Fig. 1 is employed in the numerical calculation and measurement. To study the nonlinear effects on the acoustic field parameters, we use a dimensionless nonlinear parameter N, which is defined as $N=d/l_d$. The nonlinear parameter N, which is proportional to the source amplitude, is varied from 0 to 0.44, corresponding to the focal intensity up to $3.927\times10^4\,\mathrm{W/cm^2}$. The distilled water is used as the propagation medium, with the sound velocity $c_0=1500\,\mathrm{m/s}$, density $\rho_0=1000\,\mathrm{kg/m^3}$, acoustic nonlinear coefficient $\beta=3.5$, and attenuation coefficient $\alpha_0=0.0253\,\mathrm{Np/m}$ at 1 MHz with a frequency dependence f^2.[8] For the purpose of numerical calculation and comparison of results, it is convenient to introduce the dimensionless parameters ξ (normalized axial distance) defined by $\xi=\sigma/\sigma_{\max}$, where $\sigma_{\max}=4$, corresponding to d in the rectangular coordinate. The geometrical focal point is always located at $\xi=0$ and the value of ξ varies from -1 to 1. Numerical calculation is performed by means of an implicit backward finite difference algorithm. For ensuring the reasonable accuracy, the step size of θ is set to 2.618×10^{-3} rad, the step size of σ varies with $1+\sigma^2$ and the initial size is 6.64×10^{-4}, and the maximum harmonic number is 200.

In the simulation, we first describe the change of waveform during sound propagation. Figure 2 shows the two periods of a predicted waveform at various distances in the sound axis when $N=0.1218$, i.e. in front of the focus ($\xi=-0.75$ and -0.4), at the focus ($\xi=0$) and after the focus ($\xi=0.7$). With the increase of the sound propagation distance, the waveform is gradually distorted and the peak positive pressure increases. The formation of the shock fronts is obviously seen at the focus of the ultrasound field, where the effective transition of the wave energy into heat will occur. Beyond the focus, the peak positive

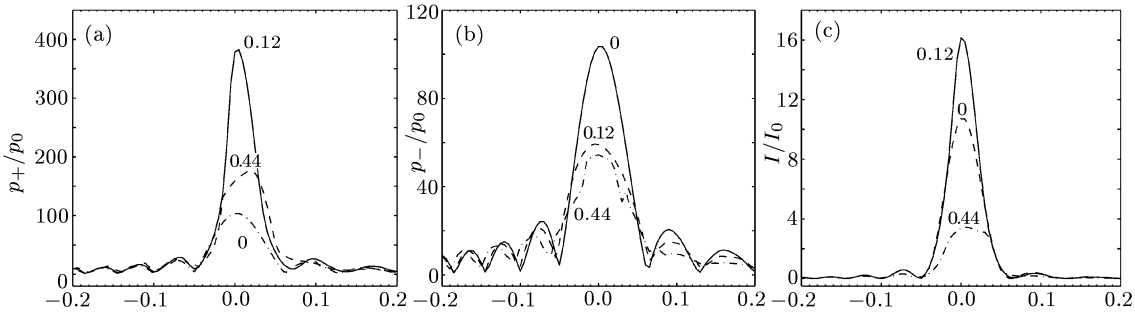

Fig. 3. Axial distributions of normalized peak positive pressure p_+, peak negative pressure p_- and intensity I in the cases of $N = 0$, 0.12 and 0.44.

pressure amplitude obviously decreases as shown in Fig. 2(d).

The most important characteristics of the acoustic field for HIFU therapy are the peak positive pressure, peak negative pressure and intensity. Nonlinear propagation and wave distortion can have a significant effect on these distributions. Figure 3 compares the axial distributions for three different values of the nonlinear parameter, i.e. $N = 0$, 0.12 and 0.44. Each graph in the figure has a unique vertical scale. It is observed that the focusing gains of the acoustical field vary differently with the increase of the value of the nonlinear parameter N. In Fig. 3(a), the linear focusing gain of p_+/p_0 is about 103.5 for the case of linear sound propagation ($N = 0$). For the case of $N = 0.12$, the focusing gain of p_+/p_0 is increased to about 370.455 owing to the nonlinear enhancement. For the case of $N = 0.44$, the focusing gain of p_+/p_0 decreases to about 176.114 due to absorption of energy on the shocks on the way to the focus. The focusing gain of intensity exhibits the similar non-monotone behaviour with the peak positive pressure, as shown in Fig. 3(c). However, the focusing gain of the peak negative pressure shows different behaviour. It monotonically decreases with the increasing value of N, as shown in Fig. 3(b).

In Fig. 4, the focusing gain of intensity as a function of the nonlinear parameter N is shown by the solid line. Each value represents the unique normalized intensity $I/I_{\max}$. As can be seen, as the nonlinearity increases, the theoretical focusing gain starts from $0.6846 I_{\max}$ ($892.6\,\mathrm{w/cm^2}$) at $N = 0$, climbs to a peak at $N = 0.1218$ ($3.927 \times 10^4\,\mathrm{W/cm^2}$), and then falls. The value is even lower than the initial value when N is larger than 0.1975. The results suggest that higher source output does not correspond to the higher output at the focus and that there exists a saturation level of source output.

To examine the validity of the numerical calculations, we measure the change of the axial intensity as a function of the nonlinear parameter N. In the experiment, a programmable function generator (Agilent 33250, USA) transmits a 1-MHz tone-burst signal (4 cycles at a period repetition frequency 100 Hz). The tone-burst signal is amplified by a broadband power amplifier (ENI A-150, USA) and used to drive the transmitter. The acoustic signal after propagating through the medium (distilled water) is detected by a broadband needle hydrophone (NP1000, USA) and sent to a digital oscilloscope (Agilent 54831, USA) for digitizing. The receiver mounted on a two-dimensional mechanical scanning unit (Newport MM3000, USA) can move along or normal to the acoustic axis with accuracy 1 μm. The receiver is located at the position where the amplitude of the pressure reaches the maximum. The change of the nonlinear parameter N is carried out by adjusting the source output. Prior to the measurement, the signal near the surface of the transmitter is measured. It is found that the waveform is almost sinusoidal, which suggests that the nonlinearity due to the transducer can be ignored. The measured normalized axial intensity is shown by circles in Fig. 4. The measured results are in agreement with the calculation.

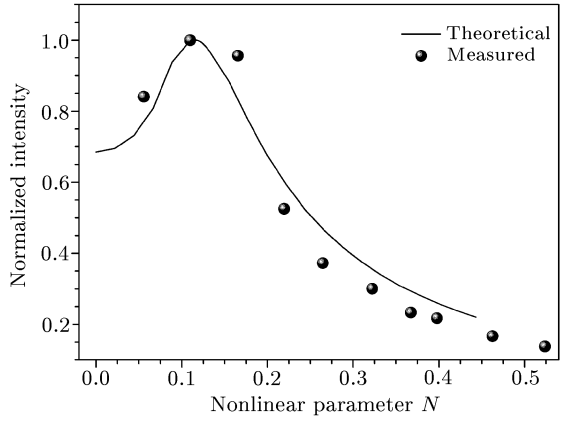

Fig. 4. Nonlinear dependence of axial normalized intensity.

In the HIFU therapy, the efficiency of thermal or mechanical impact of ultrasound on tissues is associated with the combined effects of nonlinearity and

diffraction. For better understanding of the nonlinear effects on the parameters of acoustic field, we also calculate the spatial distributions of the focusing gains of peak positive pressure, peak negative pressure and intensity as shown in Fig. 5, where abscissa denotes the θ axis and ordinate denotes the ξ axis. The patterns in this figure are presented in grey scale with 16 levels changing linearly from zero to the maximum amplitude of the corresponding parameter. For the linear beam ($N = 0$), the distributions of peak positive and negative pressures, and the intensity are shown in Figs. 5(a)–5(c). In this case, the peak positive and negative pressure distributions have the identical spatial structures. The corresponding spatial structures for $N = 0.12$ are plotted in Figs. 5(d)–5(f). Compared with the linear case, the peak positive pressure distribution is more localized in the focal region. This means that the harmonic contents result in effective beam narrowing, and that greater heating would be produced only at the fundamental frequency. On the contrary, the focal area of the peak negative pressure is noticeably displaced towards the source and is much less localized in space, especially in the direction across the beam. Figures 5 (g)–5(i) show the distributions of peak positive and negative pressures

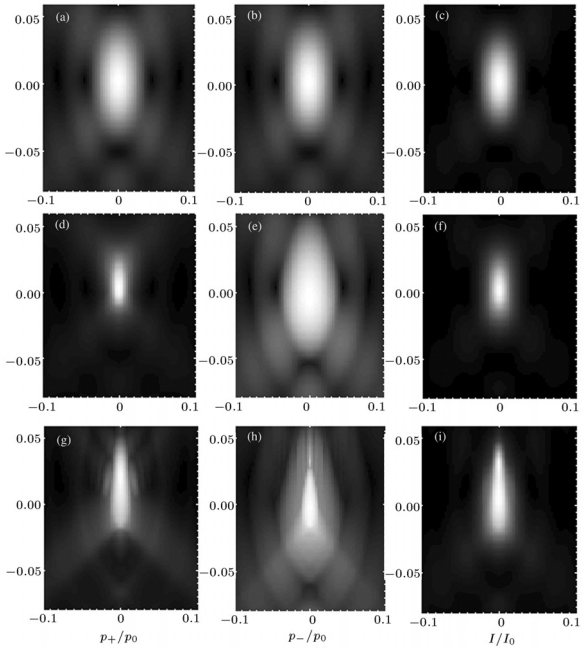

Fig. 5. Spatial distributions of normalized peak positive pressure p_+, peak negative pressure p_-, and intensity I for $N = 0$, 0.12 and 0.44.

and intensity for the case of $N = 0.44$. In this case, the peak positive pressure and intensity are less localized compared with the case of $N = 0.12$. Additionally the focal region of the three acoustic parameters changes from an ellipse to a tadpole shape. As we know, the thermal effect depends on the absorption of the wave energy on the shocks that is related to the peak positive pressure, while the cavitation effect is determined by the negative phase of the waveform. The results suggest that in the powerful focused fields, the cavitational phenomena will be pronounced in essentially wider area in comparison with the thermal effects, and the super-fast local overheating of tissue up to very high temperature is possible.

In conclusion, on the base of the nonlinear SBE equation, we have quantitatively studied the nonlinear effect on the nonlinear acoustic field radiated from a focused transducer with a wide aperture angle of 35°. Because of the combined effect of diffraction and nonlinearity, the waveform at the focus is distorted. With the increase of nonlinearity, both the peak positive pressure and the intensity start to climb a peak, and then fall; but the peak negative pressure monotonically decreases. Therefore, the efficiency of HIFU therapy can be improved by optimizing the nonlinear focusing gain. Additionally, owing to the combined effects of nonlinearity and diffraction, the acoustical field exhibits an asymmetric structure. The thermal effect caused by the peak positive pressure is more local than the cavitation effect determined by the peak negative pressure.

References

[1] ter Haar G R 1995 *Ultrasound Med. Biol.* **21** 1089
[2] Malcolm A L and ter Haar G R 1996 *Ultrasound Med. Biol.* **22** 659
[3] Kamakura T, Ishiwata T and Matsuda K 2000 *J. Acoust. Soc. Am.* **107** 3035
[4] Sun M, Zhang D and Gong X F 2006 *Chin. Phys. Lett.* **23** 649
[5] Tjøtta J N, Tjøtta S and Vefring E H 1991 *J. Acoust. Soc. Am.* **89** 1017
[6] Curra F P, Mourad P D, Khokhlova V A, Cleveland R O and Crum L A 2000 *IEEE UFFC* **47** 1077
[7] Hamilton M F and Khokhlova V A 1996 *J. Acoust. Soc. Am.* **101** 1298
[8] Khokhlova V A and Souchon R 2001 *J. Acoust. Soc. Am.* **110** 95